Highly tolerant a-Si distributed Bragg reflector fabricated by oblique angle deposition

Sung Jun Jang[1], Young Min Song[1], Chan Il Yeo[1], Chang Young Park[1], and Yong Tak Lee[1,2,3,*]

[1]School of Information and Communications, Gwangju Institute of Science and Technology, 1 Oryong-dong, Buk-gu, Gwangju, 500-712, Korea
[2]Graduate Program of Photonics and Applied Physics, Gwangju Institute of Science and Technology, 1 Oryong-dong, Buk-gu, Gwangju, 500-712 Korea
[3]Department of Nanobio Electronics and Materials, Gwangju Institute of Science and Technology,1 Oryong-dong, Buk-gu, Gwangju, 500-712, Korea
**ytlee@gist.ac.kr*

Abstract: We demonstrate a highly tolerant and highly reflective broadband a-Si distributed Bragg reflector fabricated by oblique angle deposition. By tuning the refractive index of an a-Si film, a high index contrast material system was achieved. The highly tolerant and broadband reflective characteristics of the a-Si distributed Bragg reflector were investigated by calculation and fabrication. A broad stop band ($\Delta\lambda/\lambda$ = 33.7%, R>99%) with only a five-pair a-Si distributed Bragg reflector was achieved experimentally. The size-, feature- and substrate-independent method for highly reflective Bragg reflectors was realized by simple oblique angle evaporation.

OCIS codes: (230.1480) Bragg reflectors; (310.1860) Deposition and fabrication; (220.4241) Nanostructure fabrication; (310.4165) Multilayer design.

References and links

1. M. C. Y. Huang, Y. Zhou, and C. J. Chang-hasnain, "A surface-emitting laser incorporating a high-index-contrast subwavelength grating," Nat. Photonics **1**(2), 119–122 (2007).
2. L. Zeng, P. Bermel, Y. Yi, B. A. Alamariu, K. A. Broderick, J. Liu, C. Hong, X. Duan, J. Joannopoulos, and L. C. Kimerling, "Demonstration of enhanced absorption in thin film Si solar cells with textured photonic crystal back reflector," Appl. Phys. Lett. **93**(22), 221105 (2008).
3. M. J. Thorpe, K. D. Moll, R. J. Jones, B. Safdi, and J. Ye, "Broadband cavity ringdown spectroscopy for sensitive and rapid molecular detection," Science **311**(5767), 1595–1599 (2006).
4. S. N. Tandon, J. T. Gopinath, H. M. Shen, G. S. Petrich, L. A. Kolodziejski, F. X. Kärtner, and E. P. Ippen, "Large-area broadband saturable Bragg reflectors by use of oxidized AlAs," Opt. Lett. **29**(21), 2551–2553 (2004).
5. J. Boucart, C. Starck, F. Gaborit, A. Plais, N. Bouche, E. Derouin, J. C. Remy, J. Bonnet-Gamard, L. Goldstein, C. Fortin, D. Carpentier, P. Salet, F. Brillouet, and J. Jacquet, "Metamorphic DBR and tunnel-junction injection: A CW RT monolithic long-wavelength VCSEL," IEEE J. Sel. Top. Quantum Electron. **5**(3), 520–529 (1999).
6. D. J. Ripin, J. T. Gopinath, H. M. Shen, A. A. Erchak, G. S. Petrich, L. A. Kolodziejski, F. X. Kartner, and E. P. Ippen, "Oxidized GaAs/AlAs mirror with a quantum-well saturable absorber for ultrashort-pulse Cr^{4+}:YAG laser," Opt. Commun. **214**(1-6), 285–289 (2002).
7. E. F. Schubert, N. E. J. Hunt, A. M. Vredenberg, T. D. Harris, J. M. Poate, D. C. Jacobson, Y. H. Wong, and G. J. Zydzik, "Enhanced photoluminescence by resonant absorption in Er-doped SiO_2/Si microcavities," Appl. Phys. Lett. **63**(19), 2603–2605 (1993).
8. Y. H. Lin, C. L. Wu, Y. H. Pai, and G. R. Lin, "A 533-nm self-luminescent Si-rich SiNx/SiOx distributed Bragg reflector," Opt. Express **19**(7), 6563–6570 (2011).
9. G. Zalczer, O. Thomas, J. P. Piel, and J. L. Stehle, "IR spectroscopic ellipsometry: instrumentation and applications in semiconductors," Thin Solid Films **234**(1-2), 356–362 (1993).
10. C. Mazzoleni and L. Pavesi, "Application to optical components of dielectric porous silicon multilayers," Appl. Phys. Lett. **67**(20), 2983–2985 (1995).
11. M. J. Brett and M. M. Hawkeye, "Materials science. New materials at a glance," Science **319**(5867), 1192–1193 (2008).
12. J. Q. Xi, M. F. Schubert, J. K. Kim, E. F. Schubert, M. Chen, S. Y. Lin, W. Liu, and J. A. Smart, "Optical thin-film materials with low refractive index for broadband elimination of Fresnel reflection," Nat. Photonics **1**, 176–179 (2007).

#145966 - $15.00 USD Received 20 Apr 2011; revised 16 Jun 2011; accepted 22 Jun 2011; published 24 Jun 2011

13. J. K. Kim, T. Gessmann, E. F. Schubert, J. Q. Xi, H. Luo, J. Cho, C. Sone, and Y. Park, "GaInN light-emitting diode with conductive omnidirectional reflector having a low-refractive-index indium-tin oxide layer," Appl. Phys. Lett. **88**(1), 013501 (2006).
14. M. F. Schubert, J. Q. Xi, J. K. Kim, and E. F. Schubert, "Distributed Bragg reflector consisting of high- and low-refractive-index thin film layers made of the same material," Appl. Phys. Lett. **90**(14), 141115 (2007).
15. M. M. Hawkeye and M. J. Brett, "Narrow bandpass optical filters fabricated with one-dimensionally periodic inhomogeneous thin films," J. Appl. Phys. **100**(4), 044322 (2006).
16. Y. Zhong, Y. C. Shin, C. M. Kim, B. G. Lee, E. H. Kim, Y. J. Park, K. M. A. Sobahan, C. K. Hwangbo, Y. P. Lee, and T. G. Kim, "Optical and electrical properties of indium tin oxide thin films with tilted and spiral microstructures prepared by oblique angle deposition," J. Mater. Res. **23**(09), 2500–2505 (2008).
17. K. Robbie and M. J. Brett, "Sculptured thin films and glancing angle deposition: Growth mechanics and applications," J. Vac. Sci. Technol. A **15**(3), 1460–1465 (1997).
18. S. J. Jang, Y. M. Song, H. J. Choi, J. S. Yu, and Y. T. Lee, "Structural and optical properties of silicon by tilted angle evaporation," Surf. Coat. Tech. **205**, S447–S450 (2010).
19. O. Bisi, S. Ossicini, and L. Pavesi, "Porous silicon: a quantum sponge structure for silicon based optoelectronics," Surf. Sci. Rep. **38**(1-3), 1–126 (2000).
20. J. P. Singh, T. Karabacak, D.-X. Ye, D.-L. Liu, C. Picu, T.-M. Lu, and G.-C. Wang, "Physical properties of nanostructures grown by oblique angle deposition," J. Vac. Sci. Technol. B **23**(5), 2114–2121 (2005).
21. Y. M. Song, H. J. Choi, J. S. Yu, and Y. T. Lee, "Design of highly transparent glasses with broadband antireflective subwavelength structures," Opt. Express **18**(12), 13063–13071 (2010).
22. S. Chhajed, M. F. Schubert, J. K. Kim, and E. F. Schubert, "Nanostructured multilayer graded-index antireflection coating for Si solar cells with broadband and omnidirectional characteristics," Appl. Phys. Lett. **93**(25), 251108 (2008).
23. J. Fan, J. Fu, A. Collins, and Y. Zhao, "The effect of the shape of nanorod arrays on the nanocarpet effect," Nanotechnology **19**(4), 045713–045721 (2008).
24. S. J. Jang, Y. M. Song, J. S. Yu, C. I. Yeo, and Y. T. Lee, "Antireflective properties of porous Si nanocolumnar structures with graded refractive index layers," Opt. Lett. **36**(2), 253–255 (2011).
25. S. J. Jang, Y. M. Song, C. I. Yeo, C. Y. Park, J. S. Yu, and Y. T. Lee, "Antireflective property of thin film a-Si solar cell structures with graded refractive index structure," Opt. Express **19**(S2 Suppl 2), A108–A117 (2011).
26. C. F. R. Mateus, M. C. Y. Huang, L. Chen, C. J. Chang-Hasnain, and Y. Suzuki, "Broad-band mirror (1.12-1.62 μm) using a subwavelength grating," IEEE Photon. Technol. Lett. **16**(7), 1676–1678 (2004).
27. L. Zeng, Y. Yi, C. Hong, J. Liu, N. Feng, X. Duan, L. C. Kimerling, and B. A. Alamariu, "Efficiency enhancement in Si solar cells by textured photonic crystal back reflector," Appl. Phys. Lett. **89**(11), 111111 (2006).
28. O. Blum, I. J. Fritz, L. R. Dawson, A. J. Howard, T. J. Headley, J. F. Klem, and T. J. Drummond, "Highly reflective, long wavelength AlAsSb/GaAsSb distributed Bragg reflector grown by molecular beam epitaxy on InP substrate," Appl. Phys. Lett. **66**(3), 329–331 (1995).

1. Introduction

Broadband high reflective distributed Bragg reflectors (DBRs) are essential in optical devices, including telecommunication, semiconductor lasers, solar cells, optical sensors, and photo detectors [1–4]. For DBRs, the reflectivity and stop band width directly depend on the refractive index contrast between the high- and low-index material, i.e., a higher refractive index contrast contributes to a higher reflectivity and a wider stop band. Moreover, a higher index contrast guarantees higher tolerance during the fabrication process of DBRs in the cases of permissible deviation of stop band width. Because process parameters such as the deposition rate seriously affect the quality of thin film optical components, highly tolerant DBRs are prerequisite to low-cost fabrication. Thus far, various material systems or novel techniques have been used to realize broadband high-reflective DBRs; however, these have their own limitations, including, 1) the necessity for expensive equipment and a substrate-sensitive process, 2) a complicated and protracted process, 3) non-conductive and poor thermal properties, and 4) low refractive index contrast [5–8]. Moreover, these material systems are heterostructures, as DBRs generally consist of several pairs of different materials with different refractive indices. However, the refractive index and other properties of this type of material, such as conductivity and thermal expansion coefficient are in general inseparably coupled. Due to the limited number of available materials, the choice of the refractive index also dictates the remaining material characteristics. Although porous silicon multilayers were reported in the early 1990s for a homogeneous material system, it has been limited by process tolerances, e.g. etch rate and process temperature [9,10].

Recently, it was shown that oblique-angle deposition (OAD) of materials, e.g., SiO_2, TiO_2 and ITO, can be used to fabricate optical components with optical properties that can be

#145966 - $15.00 USD Received 20 Apr 2011; revised 16 Jun 2011; accepted 22 Jun 2011; published 24 Jun 2011

controlled by the oblique angle [11–13]. By controlling the angle of deposition and thereby the layer porosity and refractive index, oblique-angle deposition allows the fabrication of thin film optical components composed of a single material chosen for its optical properties in which each layer has a different refractive index that is individually tuned to a specific desired value. Schubert et al. reported experimental results involving a homogeneous DBR structure by OAD but the index contrast was still low [14]. The capability of the use of a single-step and single-material deposition for high-low or graded-index optical component is crucial when a highly tolerant process is important [15].

This paper represents the first-demonstration of amorphous silicon (a-Si) DBRs fabricated by OAD having high process tolerance and broadband high-reflective properties due to the high index contrast. A five-period a-Si/a-Si DBR was fabricated by OAD via e-beam evaporation on a two-inch silicon wafer (100). The reflectivity and wafer-scale uniformity were analyzed by spectrophotometry measurements and reflectivity mapping. This a-Si/a-Si DBR has advantages in that it offers the least complicated means of realizing a highly tolerant and large-scale mirror fabrication process leading to high reflectivity with a wide stop band.

2. Design and Fabrication

To realize an a-Si/a-Si DBR, the low- and high-index layers of the a-Si should be prepared with high refractive index contrast. The Si layers were deposited on Si substrate by an e-beam evaporator using inclined sample holders for the tilted angle evaporation. A detail discussion about the experimental setup was reported in a previous paper [16]. Generally, the refractive index of the deposited film decreases as the oblique angle increases in the OAD process [16,17]. This means that the most oblique angle is necessary for the highest index contrast. However, excessively tilted evaporation creates a roughened surface on the deposited film and porous structure that can be filled by subsequently arriving atoms for the high index layer [14]. Therefore, a carefully chosen oblique angle and refractive index for the low index layer are crucial to ensure a high index contrast DBR by OAD.

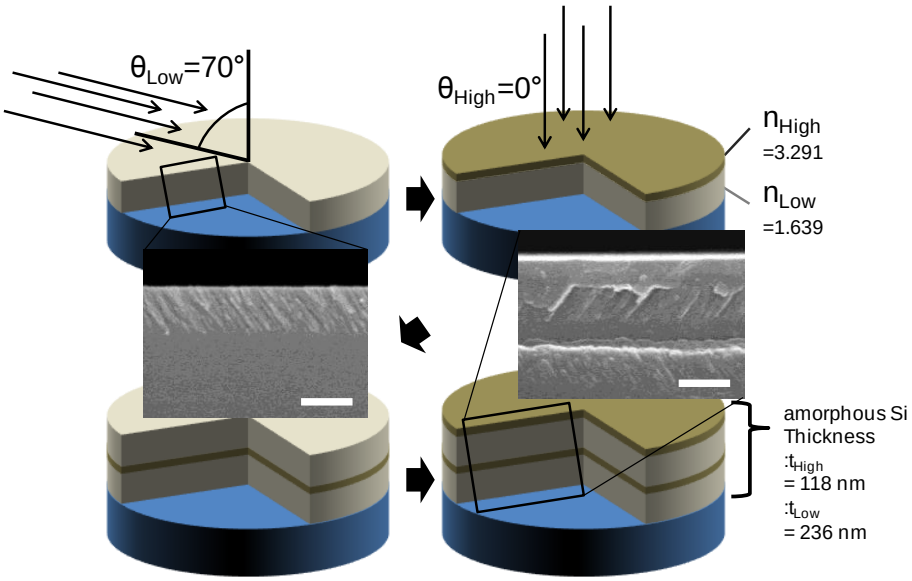

Fig. 1. Schematic diagrams of the fabrication process steps and SEM images of a-Si DBR structure based on OAD. Scale bars: 100 nm.

A schematic of the fabrication procedure is shown in Fig. 1. Normally high reflective DBRs consist of low-index layers alternatively with high-index layers. Initially, a low-index layer was deposited by OAD with a tilted angle of 70°, which was carefully chosen from the results of previous work [18]. As shown in a cross-sectional scanning electron microscopic

#145966 - $15.00 USD Received 20 Apr 2011; revised 16 Jun 2011; accepted 22 Jun 2011; published 24 Jun 2011

(SEM) image in Fig. 1, the nanocolumnar layer has the distinct pattern of a vacancy; hence, the refractive index of the layer was decreased by a controllable amount. The refractive index of a nanocolumnar material is determined by the volume fractions of the air and the material. For two parameters with volume fractions of V_{air} and $V_{a\text{-}Si}$, where $V_{air} + V_{a\text{-}Si} = 1.0$, and refractive indices n_{air} and $n_{a\text{-}Si}$, the Bruggemann effective medium approximation is

$$V_{air}\left(n_{air}-n_{eff}^2\right)\Big/\left(n_{air}+2n_{eff}^2\right)+\left(1-V_{air}\right)\left(n_{a-Si}^2-n_{eff}^2\right)\Big/\left(n_{a-Si}^2+2n_{eff}^2\right)=0\,, \quad (1)$$

where n_{eff} is the effective refractive index of the nanocolumnar a-Si film and V_{air} is the volume fraction of air (or the porosity of the film) [19]. The porosity V_{air} of the low-n a-Si layer was calculated to be 65.5% using the following parameters: $n_{eff} = 1.639$, $n_{a\text{-}Si} = 3.291$, and $n_{air} = 1.0$. The characterization of the mechanical, electromechanical, thermal and other physical properties of nanostructured Si films has already been presented [20]. The porous Si films seem fragile, but even in the conventional semiconductor process it can stand without any physical or optical changes. Secondly, as a high refractive index layer, the a-Si film was deposited with normal incident e-beam flux. Because our first deposited low-index layer has a relatively flat surface, we could ignore the filling in of certain spaces between the nanocolumns. Figure 2 shows the results of cross-sectional SEM and transmission electron microscopic (TEM) measurements of the fabricated five-period a-Si/a-Si DBR. As shown in Fig. 2 (a), the fabricated five-period a-Si/a-Si DBR was precisely formed on a silicon substrate (100) by OAD. For the low-index layer and the high-index layer, the tilted e-beam flux was fixed respectively at 70° and 0°, as mentioned above. The gap between the nanocolumnar structures is less than 10 nm, i.e., much smaller than the wavelength of visible light, thereby limiting optical scattering [21]. In this case, the SEM is not well suited for analyzing such random and nanocolumnar structures, especially the interface between low and high refractive index layers. Hence, we used the TEM image in Fig. 2 (b). Normally, a film deposited at an oblique angle has significant porosity, leading to an uneven surface [22,23]. Nevertheless, the interface between the low- and high-index layers is relatively good to distinguish the interfaces in this work, as depicted in the TEM image. The estimated thicknesses of the low- and high-index layers are 220 ± 5 nm and 118 ± 2 nm, respectively. While the normal deposition was precisely controllable, the OAD had a thickness error of approximately 10 nm. The thickness error of the OAD a-Si film may result from the estimation error of the deposition rate of the OAD. Notwithstanding this, as the film was deposited by evaporation, the controllability of the film thickness was mostly suitable for quarter-wavelength optical films.

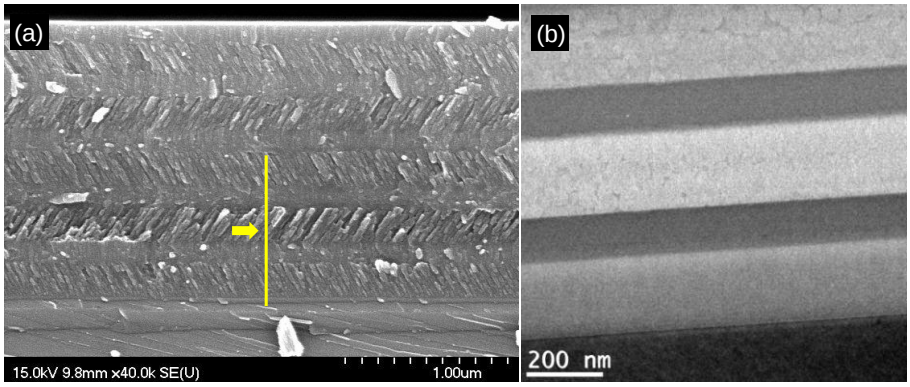

Fig. 2. (a) SEM image of 5 period a-Si/a-Si DBR fabricated on Si substrate. The yellow line is a cross-section for an image enlarged by TEM, and the image of a-Si DBR is shown in (b).

#145966 - $15.00 USD Received 20 Apr 2011; revised 16 Jun 2011; accepted 22 Jun 2011; published 24 Jun 2011

3. Results and Discussion

The reflective property of the five-period a-Si/a-Si DBR structure was investigated both theoretically and experimentally. The calculated and measured reflective spectra are shown in Fig. 3 (a) and (b), respectively. For comparison, the reflectivity values of DBRs with other general material systems were calculated, with these results shown in Fig. 3 (a). The reflectance calculation was done using a method based on a rigorous coupled-wave analysis (RCWA), and each material property of the a-Si films was sourced from previous results [18,24,25]. The highest reflectivity, close to 100%, was observed in the wavelength range from 1400 nm to 1800 nm, and nearly perfect agreement between the calculated and measured results was observed. In addition, the stop band with high reflectivity ($\Delta\lambda/\lambda$, R>99%) of the a-Si/a-Si DBR was comparable to the other material systems in both the experimental and calculated results, as shown in Table 1. The stop band from the measured result is comparable to that of subwavelength gratings designed with a high level precision [26]. This may be contributed by the large index contrast [27,28]. Figure 3 (b) shows the reflectivity spectra of fabricated a-Si/a-Si DBRs as a function of the number of periods. A three-period a-Si/a-Si DBR was sufficient to ensure high reflectivity that exceeded 97%.

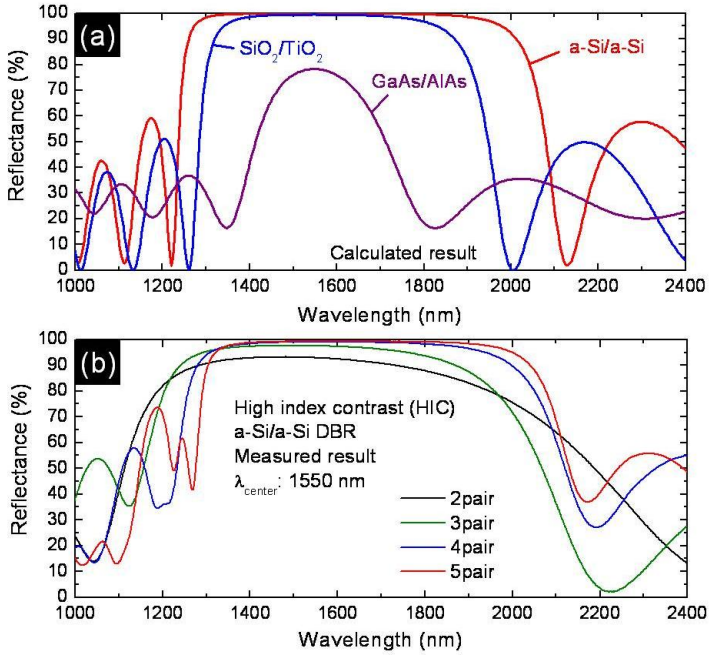

Fig. 3. (a) Calculated reflectivity spectra of GaAs/AlAs, SiO_2/TiO_2 and a-Si/a-Si DBRs as a function of wavelength. (b) Measured reflectivity spectra of 2, 3, 4 and 5 period a-Si/a-Si DBRs as a function of wavelength. The center wavelength of every DBR was 1550 nm.

Table 1. Refractive index, thickness, index contrast and stop bandwidth of GaAs/AlAs, SiO_2/TiO_2 and a-Si/a-Si DBRs. The center wavelength is 1550 nm.

(λ_c~1550 nm)

	n_{low}	n_{high}	t_{low}	t_{high}	Δn	$\Delta\lambda/\lambda_c$ (R>99%)
GaAs/AlAs	2.894	3.374	134 nm	115 nm	0.480	0%
SiO_2/TiO_2	1.444	2.447	268 nm	158 nm	1.003	16.6%
a-Si/a-Si (Cal)	1.639	3.291	236 nm	118 nm	1.652	35.6%
a-Si/a-Si (Exp)	-	-	220 ± 5 nm	118 ± 2 nm	-	33.7%

#145966 - $15.00 USD Received 20 Apr 2011; revised 16 Jun 2011; accepted 22 Jun 2011; published 24 Jun 2011

To demonstrate the high process tolerance and potential for a large-scale process, we fabricated a 2" full-wafer a-Si/a-Si DBR with five periods. The result from the reflectivity mapping of the 2" full-wafer a-Si/a-Si DBR is shown in Fig. 4 (a). The relative reflectivity map was measured by reflectance mapping tool (RPM 2000, Nanometrics) at the center wavelength of 1550 nm. There is a slightly different color in the measured relative reflectivity, as the wafer was not rotated in the evaporating chamber. This indicates that the evaporating distance to one edge of the wafer is slightly different from the distance to the opposite edge. Nevertheless, relatively uniform reflectivity of the full-wafer DBR was achieved. To study the influence of the sample position on the reflectivity, we measured the reflectivity of each position marked in Fig. 4 (a) by spectrophotometry measurement. As shown in Fig. 4 (b), there was little difference in the measured reflectivity of each position. Furthermore, the calculated results shown in Fig. 5 show that a certain amount of thickness deviation does not have a serious effect on the reflectivity of the a-Si/a-Si DBR at the target wavelength. This is also true for the circumferential wavelength. In Fig. 4 (b), the largest difference exists between B and E. The wavelength difference of spectral band width between B and E was about 45 nm. We can define the thickness errors of position B and E from Fig. 5. They were −5 nm and −1 nm respectively, and the total deviation across the whole wafer was only 4 nm. Therefore, the DBRs oblique angle deposited on 2" wafer show relatively good uniformity. Therefore, we can indeed confirm that the highly tolerant and high reflective a-Si/a-Si DBR is useful, practical and innovative for cost-effective optical components capable of high levels of reflection.

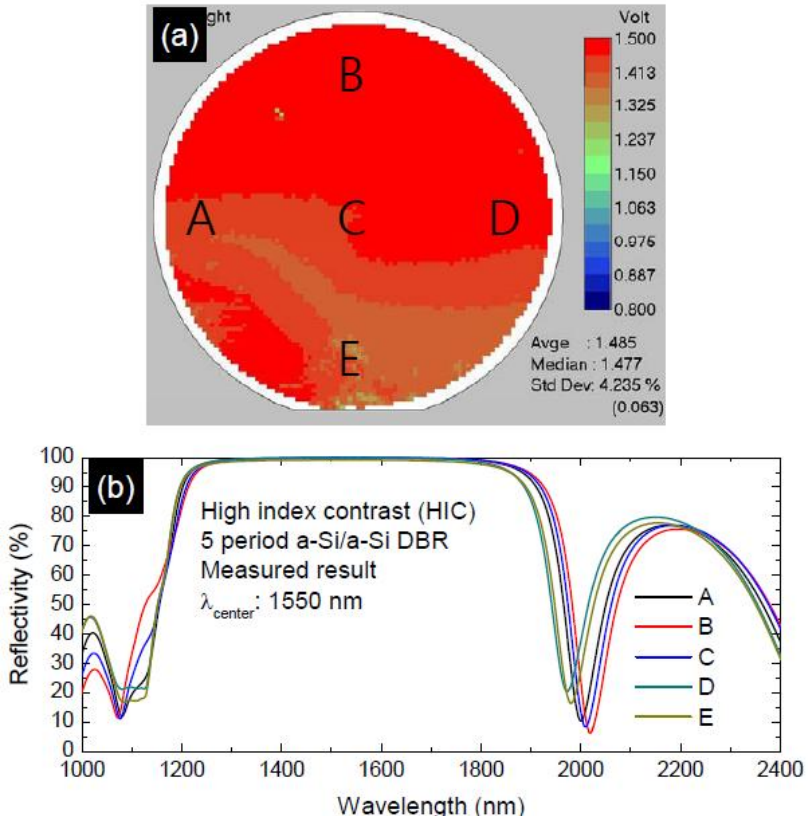

Fig. 4. (a) The relative reflectance mapping image of 2" full-wafer DBR fabricated on Si substrate. The words, A-E, represent each measurement position for the reflectivity. (b) The measured reflectivity of all positions of DBR fabricated on 2" Si wafer as a function of wavelength.

#145966 - $15.00 USD Received 20 Apr 2011; revised 16 Jun 2011; accepted 22 Jun 2011; published 24 Jun 2011

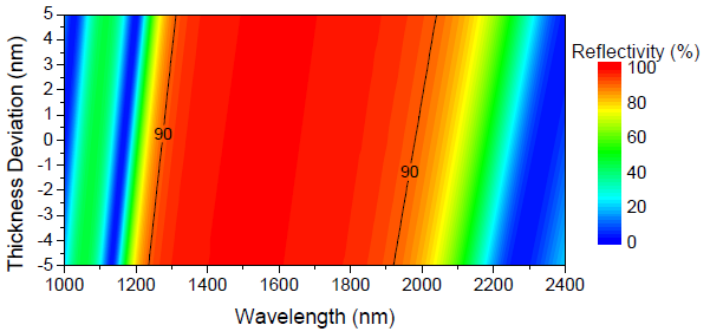

Fig. 5. Calculated reflectivity spectra and thickness deviation dependency of the five-period a-Si/a-Si DBR as a function of wavelength.

Figure 6 (a) shows a digital photographic image of the deposited a-Si/a-Si DBR shaped as the media mark of an institute. Any size or any feature of a structure can be fabricated by a simple lift-off process for the realization of a highly reflective broadband DBR suitable for various optoelectronic devices. As shown in Fig. 6 (b), the relative reflectivity of the patterned structure at 1550 nm was plainly higher than that of a normal Si (100) substrate and the superiority of the tolerant a-Si/a-Si DBR and its fabrication process are clearly evident.

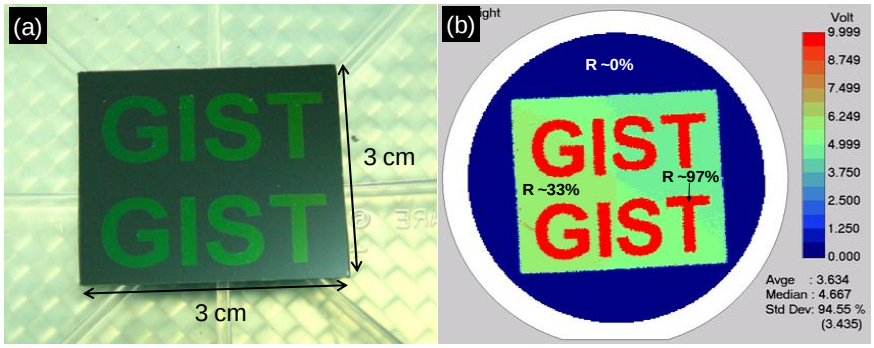

Fig. 6. (a) Photographic image of 'GIST'-patterned a-Si/a-Si DBR on Si substrate. (b) Relative reflectance mapping image of 'GIST'-patterned a-Si/a-Si DBR on Si substrate.

4. Conclusion

In summary, we proposed a novel class of DBRs based the OAD of a-Si. The reflective characteristics were investigated both theoretically and experimentally. Highly tolerant and highly reflective broadband a-Si/a-Si DBRs were demonstrated successfully for the first time. A broadband stop band ($\Delta\lambda/\lambda$ = 33.7%, R>99%) with only a five-period a-Si/a-Si DBR was achieved experimentally. The size-, feature- and substrate-independent method to realize highly tolerant and broadband DBRs will provide an interesting new pathway that opens future practical applications such as resonant-cavity-light-emitting-diodes or vertical-cavity-surface-emitting-lasers or solar cells. In an addition, oblique-angle deposition is promising for the growth of homogeneous highly reflective DBR structures with a very high refractive index contrast.

Acknowledgments

This work was partially supported by the "Systems biology infrastructure establishment grant" provided by GIST in 2011 and by the WCU program of MEST (Project No. R31-2008-000-10026-0) and by the National Research Foundation of Korea (NRF) grant funded by the Korea government (MEST) (No. 2011-0017606).

#145966 - $15.00 USD Received 20 Apr 2011; revised 16 Jun 2011; accepted 22 Jun 2011; published 24 Jun 2011